

Coherent mode-selective Raman excitation towards standoff detection

Haowen Li¹, D. Ahmasi Harris², Bingwei Xu², Paul J. Wrzesinski², Vadim V. Lozovoy² and Marcos Dantus^{2*}

¹ BioPhotonic Solutions Inc. Okemos MI 48864, USA

² Department of Chemistry, Michigan State University, East Lansing MI 48824, USA

*Corresponding author: dantus@msu.edu

Abstract: We report the detection of characteristic Raman lines for several chemicals using a single-beam coherent anti-Stokes Raman scattering (CARS) technique from a 12 meter standoff distance. Single laser shot spectra are obtained with sufficient signal to noise ratio to allow molecular identification. Background and spectroscopic discrimination are achieved through binary phase pulse shaping for optimal excitation of a single vibrational mode. These results provide a promising approach to standoff detection of chemicals, hazardous contaminants, and explosives.

©2008 Optical Society of America

OCIS codes: (300.6230) Spectroscopy, coherent anti-Stokes Raman scattering; (320.5540) Pulse shaping

References and links

1. M. Gruebele, G. Roberts, M. Dantus, R. M. Bowman, and A. H. Zewail, "Femtosecond temporal spectroscopy and direct inversion to the potential - application to iodine," *Chem. Phys. Lett.* **166**, 459-469 (1990).
2. A. M. Weiner, D. E. Leaird, G. P. Wiederrecht, and K. A. Nelson, "Femtosecond pulse sequences used for optical manipulation of molecular-motion," *Science* **247**, 1317-1319 (1990).
3. N. Dudovich, D. Oron, and Y. Silberberg, "Single-pulse coherently controlled nonlinear Raman spectroscopy and microscopy," *Nature* **418**, 512-514 (2002).
4. D. Oron, N. Dudovich, and Y. Silberberg, "Femtosecond phase-and-polarization control for background-free coherent anti-Stokes Raman spectroscopy," *Phys. Rev. Lett.* **90**, 213902 (2003).
5. S. H. Lim, A. G. Caster, and S. R. Leone, "Single-pulse phase-control interferometric coherent anti-Stokes Raman scattering spectroscopy," *Phys. Rev. A* **72**, 0418031-0418034 (2005).
6. B. von Vacano and M. Motzkus, "Time-resolved two color single-beam CARS employing supercontinuum and femtosecond pulse shaping," *Opt. Commun.* **264**, 488-493 (2006).
7. M. O. Scully, G. W. Kattawar, R. P. Lucht, T. Opatrny, H. Pilloff, A. Rebane, A. V. Sokolov, and M. S. Zubairy, "FAST CARS: Engineering a laser spectroscopic technique for rapid identification of bacterial spores," *P. Natl. Acad. Sci. USA* **99**, 10994-11001 (2002).
8. D. Pestov, R. K. Murawski, G. O. Ariunbold, X. Wang, M. C. Zhi, A. V. Sokolov, V. A. Sautenkov, Y. V. Rostovtsev, A. Dogariu, Y. Huang, and M. O. Scully, "Optimizing the laser-pulse configuration for coherent Raman spectroscopy," *Science* **316**, 265-268 (2007).
9. M. Nisoli, S. DeSilvestri, and O. Svelto, "Generation of high energy 10 fs pulses by a new pulse compression technique," *Appl. Phys. Lett.* **68**, 2793-2795 (1996).
10. L. Gallmann, T. Pfeifer, P. M. Nagel, M. J. Abel, D. M. Neumark, and S. R. Leone, "Comparison of the filamentation and the hollow-core fiber characteristics for pulse compression into the few-cycle regime," *App. Phys. B* **86**, 561-566 (2007).
11. V. V. Lozovoy, I. Pastirk, and M. Dantus, "Multiphoton intrapulse interference. 4. Characterization of the phase of ultrashort laser pulses," *Opt. Lett.* **29**, 775-777 (2004).
12. B. Xu, J. M. Gunn, J. M. Dela Cruz, V. V. Lozovoy, and M. Dantus, "Quantitative investigation of the multiphoton intrapulse interference phase scan method for simultaneous phase measurement and compensation of femtosecond laser pulses," *J. Opt. Soc. Am. B* **23**, 750-759 (2006).
13. I. Pastirk, X. Zhu, R. M. Martin, and M. Dantus, "Remote characterization and dispersion compensation of amplified shaped femtosecond pulses using MIIPS," *Opt. Express* **14**, 8885-8889 (2006).
14. D. Oron, N. Dudovich, and Y. Silberberg, "Single-pulse phase-contrast nonlinear Raman spectroscopy," *Phys. Rev. Lett.* **89**, 273001 (2002).
15. M. Comstock, V. V. Lozovoy, I. Pastirk, and M. Dantus, "Multiphoton intrapulse interference 6; binary phase shaping," *Opt. Express* **12**, 1061-1066 (2004).

16. V. V. Lozovoy, B. W. Xu, J. C. Shane, and M. Dantus, "Selective nonlinear optical excitation with pulses shaped by pseudorandom Galois fields," *Phys. Rev. A* **74**, 0418051-0418054 (2006).
17. M. R. Schroeder, *Number Theory in Science and Communication: With Applications in Cryptography, Physics, Digital Information, Computing, and Self-similarity* (Springer, Berlin, 1997), p. 362.
18. J. Knauer, "Merit factors for least autocorrelation binary sequences", retrieved http://www.chemistry.msu.edu/faculty/dantus/merit_factor_records.html.
19. A. M. Weiner, J. P. Heritage, and E. M. Kirschner, "High-resolution femtosecond pulse shaping," *J. Opt. Soc. Am. B* **5**, 1563-1572 (1988).
20. G. Varsanyi, *Vibrational Spectra of Benzene Derivatives* (Academic Press, New York, 1969).
21. J. Konradi, A. K. Singh, and A. Materny, "Selective excitation of molecular modes in a mixture by optimal control of electronically nonresonant femtosecond four-wave mixing spectroscopy," *J. Photochem. Photobiol.* **180**, 289-299 (2006).
22. This work was first presented at the CLEO/QELS conference, May 6-11, 2007.

Ultrashort pulses have made possible the development of powerful spectroscopic tools that rival conventional high-resolution approaches [1]. Their ultra-broad bandwidth makes them ideal for impulsive excitation of vibrational modes, which evolve in time coherently. When pairs or trains of such pulses are used, large amplitude molecular motion can be achieved [2]. These capabilities were recently combined to achieve single-beam coherent anti-Stokes Raman scattering microscopy [3-6], a modality that is sensitive to molecular composition. Here we present a method for remote sensing of films and residues located on solid targets tens of meters from the laser based on single-beam CARS [22]. In contrast to its implementation in microscopy, this development requires amplified (six-orders of magnitude) ultra-broad bandwidth pulses. As well as, phase and polarization pulse shaping to deliver optimally coherent pulses tens of meters from the laser source. The resulting method is capable of selective vibrational mode excitation to provide molecular discrimination and to eliminate the non-resonant contribution. The single-beam CARS method eliminates the need for crossing three separate laser pulses (pump, Stokes, and probe) as used for arms-length identification of anthrax spores [7,8], making it more practical for standoff detection 50-100 m from the laser and detection unit.

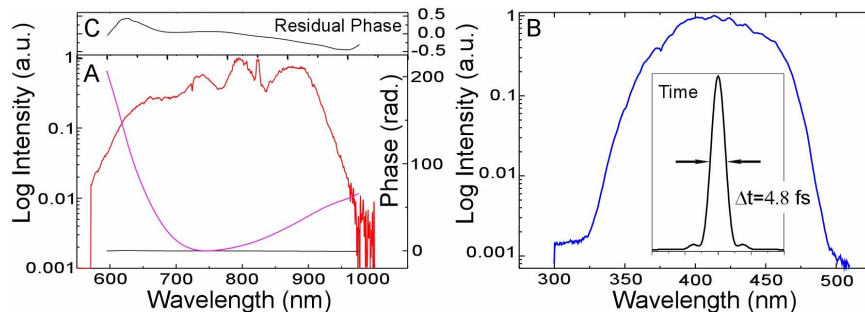


Fig. 1. (a) Supercontinuum spectrum (red) and the phase measured using MIIPS (magenta). (b) Measured SHG spectra (blue) from the compensated pulses (spectrometer limited at 300 nm). The experimental SHG spectrum has a bandwidth of 73nm (FWHM), which agrees well with simulations for transform-limited pulses based on the measured spectrum. The supercontinuum pulses were compressed to 4.8 fs by MIIPS phase compensation (see inset). (c) Residual phase on the laser after compensation.

Femtosecond laser pulses from a Mira oscillator (Coherent) are shaped by a $4f$ reflective pulse shaper using a 128-pixel phase-only programmable liquid crystal spatial light modulator (SLM) (CRi). The shaped pulses are then amplified by a regenerative amplifier (Legend USP, Coherent) and focused by a 1 meter focal length curved mirror into an argon-filled hollow waveguide that is 0.39 m long and has a 500 μm inner diameter. By adjusting the incident laser power, argon pressure and chirp of the input laser pulse, a continuum broadened spectrum is generated [9,10]. An argon pressure of 0.15 MPa with input pulse energy of 340 μJ is found to generate 200 μJ of hollow waveguide output from 750 to 870 nm.

Optimum continuum generation is obtained when high-order dispersion is eliminated by the pulse shaper using multiphoton intrapulse interference phase scan (MIIPS) [11,12] and a linear chirp of -500 fs^2 is then added to the input pulse. The broad bandwidth output laser beam is collimated by a 0.75 m focal length curved mirror and shaped by a second 4f pulse shaper with a 640-pixel, phase and polarization SLM (CRi).

The supercontinuum output spectrum is shown in Fig. 1(a); the spectral phase of the output laser beam is measured and compensated by using remote MIIPS [13], as shown in Fig. 1(c). The compensated, 4.8 fs pulses, are found to generate a very broad second harmonic generation (SHG) spectrum, shown in Fig. 1(b).

For the CARS measurements, wavelengths shorter than 765 nm are blocked at the Fourier plane of the pulse shaper. The laser beam is reflected by a beam splitter and loosely focused on the target 12 m away by a home-built Newtonian telescope consisting of a negative 0.2 m focal length lens and a 0.75 m focal length spherical curved mirror (see Fig. 2(a)). The energy at the sample is $10 \mu\text{J}/\text{pulse}$, and the beam diameter is 2 mm. This laser power is well below the damage threshold of all the samples studied. For most of the measurements presented here, a mirror is placed behind the sample to retro-reflect the CARS signal for detection through the same telescope. After the signal passes through a horizontal polarizer and a 740 nm low pass filter (Omega Optical), a compact QE65000 spectrometer (Ocean Optics) is used to record the CARS spectrum. For other measurements, we remove the mirror behind the target and applied liquid samples (toluene and *o*-xylene), which form a thin film, to a scattering surface.

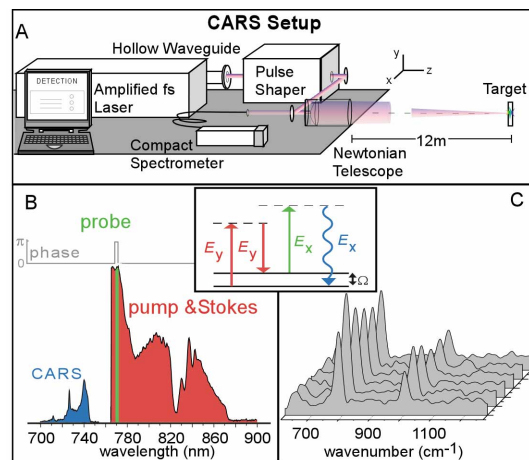


Fig.2. Setup and performance of the single-beam CARS. (a) The experimental setup. (b) The spectrum, phase and polarization of components of the shaped laser pulse. The pump and Stokes (red) components have vertical polarization (y) while the probe (green) and CARS signal (blue) have horizontal polarization (x). The inset shows a diagram for the CARS process. (c) Spectra of six consecutive single shot spectra of toluene collected at a standoff 12 m distance.

As previously mentioned, the second pulse shaper uses MIIPS to compensate the dispersion introduced by the hollow waveguide, telescope optics and propagation in air ($k_{air}'' = 20.1 \text{ fs}^2/\text{m}$) [13], ensuring transform-limited pulses at the target. It is also used to control the phase and polarization of different components of the laser pulse in a way that minimizes the non-resonant contribution and improves resolution. The non-resonant CARS signal increases with the bandwidth of the laser, which in our case is 1800 cm^{-1} . In order to reduce the considerable background in single-beam CARS microscopy Oron *et al.* use a π phase gate [14]. In other work, they have also introduced a polarization gate to the probe to further improve the resolution [4]. We incorporate both of these strategies in our approach. The probe pulse is defined by keeping 6 out of 640 pixels (about 1.5 nm bandwidth, centered

at 770 nm) horizontally polarized while using the SLM to rotate the rest of the pulse to vertical polarization. A π phase gate (3 out of 640 pixels) is also used. Single shot spectra obtained from a liquid toluene sample are shown in Fig. 2(c) to illustrate the speed, reproducibility and sensitivity of the system.

The single-beam CARS spectra of several liquid, gaseous and solid state samples obtained at a distance of 12 m are shown in Fig. 3. For these spectra, the non-resonant broad-bandwidth contribution is fitted and removed by subtraction. Figures 3(a) and 3(b) present CARS spectra for a number of liquid samples including different isomeric species, which are easily distinguishable by this technique. Spectra from carbon disulfide (CS_2), 1,2-dichloroethane ($\text{C}_2\text{H}_4\text{Cl}_2$) and chloroform (CHCl_3) vapors (0.11 m sample path length with vapor pressures of 40, 12, and 21 kPa respectively) were also recorded, and are shown in Fig. 3(c). The spectra for several solids including polycarbonate, polystyrene and polymethyl methacrylate (PMMA) are displayed in Fig. 3(c). We have observed similar signal levels for condensed phase samples of 0.1 to 10 mm thickness, leading us to believe that the majority of signal generation occurs within a thin region of the sample where phase matching is satisfied. We examined binary mixtures of *p*- and *o*-xylene, and found we could detect as little as 1% of one compound dissolved in the other (data not shown).

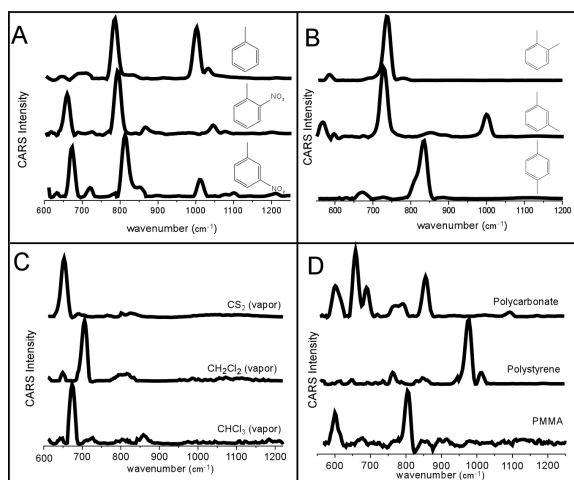


Fig. 3. Single-beam CARS spectra from liquid, gaseous and solid state samples. (a) CARS spectra from liquid toluene, *o*-nitrotoluene and *m*-nitrotoluene; (b) CARS spectra from liquid *ortho*, *meta* and *para*-xylene. (c) CARS spectra from CS_2 , CH_2Cl_2 and CHCl_3 vapors; (d) CARS spectra from solid polycarbonate, polystyrene and PMMA.

To illustrate the necessity for compensation of phase distortions, the unprocessed CARS spectrum of *m*-xylene is presented in Fig. 4(a) before and after elimination of spectral phase distortion using MIIPS, which results in a significant (order of magnitude) increase in the CARS signal. Note that despite polarization shaping, the non-resonant contribution (broad feature spanning the whole spectrum) is more intense than the resonant CARS features at 725 and 1000 cm^{-1} . The ability to isolate the desired signal from a complex chemical background is a critical requirement for molecular sensing. In particular, for CARS it is important to eliminate, as much as possible, contributions from the non-resonant contribution. These improvements are achieved by phase, amplitude and polarization shaping.

In addition to affecting the non-resonant signal, spectral phase can also provide a method for achieving molecular selectivity. Silberberg and coworkers used a sinusoidal phase function to control the single-beam, broad bandwidth CARS process and achieved molecular selectivity [3]. Also, maximum intrapulse interference can be used to achieve selectivity in nonlinear optical processes using binary phase functions [15,16]. When using binary phases, the laser pulse spectrum is partitioned into discrete regions, each receiving a phase retardation

value of zero or π . The CARS signal at each frequency Ω is given by the sum of discrete contributions from all the frequencies in the pulse whose difference is Ω according to the equation: $E(\Omega) = \sum_{\omega} E(\omega)E^*(\omega-\Omega)$, where the electric field E can only take the value of (+1) when the phase is zero and (-1) when the phase is π . The goal becomes finding the binary phase function that causes the sum to reach a maximum for the desired Ω , and zero elsewhere. Fortunately, this problem has been solved in the field of mathematics. The type of functions that we are looking for are known as Galois fields [17], or minimum correlation sequences [18]. Pseudorandom binary sequences have been used to create pulse trains [2,19] and to control nonlinear optical processes [16].

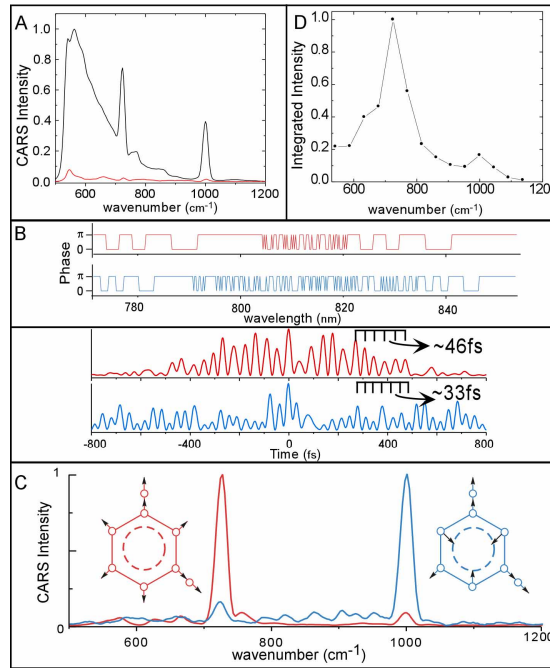


Fig. 4. Single-beam CARS illustration of sensitivity and discrimination against background signals. (a) Unprocessed spectra of *m*-xylene collected at a standoff 12 m distance with (black) and without (red) phase distortion compensation using MIIPS; note the presence of a large non-resonant contribution (compared to the resonant signal) in both cases. (b) The red phase is designed to optimize excitation of the ν_1 breathing mode at 725 cm^{-1} and the blue phase is designed to optimize excitation of ν_{12} in-plane bending mode at 1000 cm^{-1} . The lower panel shows the calculated temporal profiles corresponding to red and blue phases. (c) Unprocessed CARS spectra from *m*-xylene with two specially designed binary phases. Note that the non-resonant contribution is successfully suppressed eliminating the need for data processing. The designed binary phases control the ratio between the two Raman peaks with an overall two order-of-magnitude discrimination from 7:1 to 1:12. (d) Integrated intensity for different binary phases (optimized for different Raman shifts) applied in the pulse shaper.

Here, we use optimal discrimination based on Galois fields synthesized using binary phase functions to achieve selective excitation of individual vibrational modes, and at the same time eliminate the non-resonant contribution. One of the reasons why the non-resonant signal is greatly reduced is that the complex binary spectral phase causes the creation of a train of pulses in the time domain (see Fig. 4(b)). The temporal profiles of the pulses corresponding to red and blue binary phases show oscillation periods ~ 46 fs and ~ 33 fs, which match the vibration frequency of ν_1 breathing and ν_{12} in-plane bending modes of *m*-xylene, respectively. By spreading the peak intensity of the ultrashort pulse into several sub-pulses, the non-resonant contribution is essentially eliminated. This type of pulse shaping allows for

CARS data to be collected with high selectivity despite the ultrabroad bandwidth. The unprocessed spectra in Fig. 4(c) show selective excitation of the ν_1 or ν_{12} modes of *m*-xylene [20], with the elimination of non-resonant contribution. We point out that selective vibrational excitation of two different molecules in a mixture was reported recently using feedback-controlled optimization in a three beams (two colors) setup with a special crossed-beam geometry [21]. Frequency selective excitation, as shown here, gives single-beam CARS a means to discriminate between different compounds in a complex mixture, making it ideal for applications in complex environments. By collecting the integrated CARS signal for each binary phase, single-beam CARS spectroscopy can be achieved without a spectrometer, as shown in Fig. 4(d).

Up to this point, the data obtained made use of a mirror placed behind the sample to retro-reflect the CARS signal. In Fig. 5, we show data obtained from back-scattered signal. For this experiment, we apply a drop of toluene or *o*-xylene on a surface covered with transparent polymer beads. The signal is collected by imaging the surface on the detection fiber placed at an arms-length distance. The characteristic Raman signatures can be easily identified. As we contemplate the application of this method to standoff detection of explosives at 50-100 m, we plan to increase the energy per pulse from 10 μ J to 100 μ J, increase the diameter of the telescope used for excitation and signal collection, and to use a photon counting, spectrally dispersed signal detector. Overall, we expect these changes should result in up to three orders of magnitude increase in signal. By using the time-gated detector, we will be able to obtain time-of-arrival information of the CARS signal and to further discriminate against ambient light. With these enhancements, we believe that this approach will have a significant impact in the standoff detection of films and residues located on solid targets which scatter or reflect the incident light.

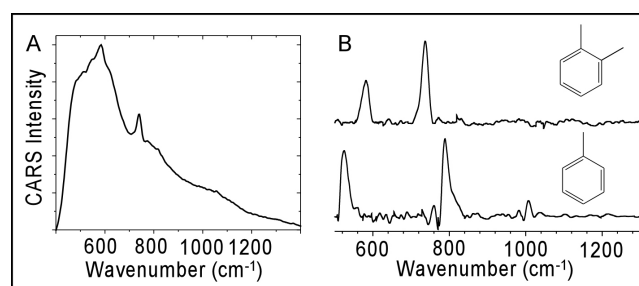


Fig. 5. Single-beam CARS spectra with back scatter signal detection. (a) Unprocessed spectrum of *o*-xylene. (b) Processed spectra of *o*-xylene and toluene.

In conclusion, coherent control over the CARS process yields the sensitivity, selectivity, background discrimination and detection speed desirable for standoff identification of compounds and mixtures as illustrated in data from several solid, liquid and gaseous samples. By delivering accurately phase-shaped ultra-broad bandwidth pulses, we can ensure maximum coherent enhancement of the signal. The gain in efficiency reduces the required laser power, resulting in a safe and non-destructive standoff detection technology. This method of frequency-selective discrimination can also be adapted for selective CARS microscopy to differentiate between different sub-cellular constituents without the need for fluorescent labeling.

Acknowledgements

Funding for this work comes from a grant to BioPhotonic Solutions Inc. and to Michigan State University from the Army Research Office. The content of the information does not necessarily reflect the position or the policy of the Government, and no official endorsement should be inferred.